Journal of Biomechanics 85 (2019) 18–26

Contents lists available at ScienceDirect

Journal of Biomechanics

journal homepage: www.elsevier.com/locate/jbiomech
www.JBiomech.com

Cervical spine morphology and ligament property variations: A finite element study of their influence on sagittal bending characteristics

Jobin D. John [a,b], Gurunathan Saravana Kumar [a,*], Narayan Yoganandan [b]

[a] Department of Engineering Design, Indian Institute of Technology Madras, India
[b] Center for NeuroTrauma Research, Department of Neurosurgery, Medical College of Wisconsin, USA

ARTICLE INFO

Article history:
Accepted 26 December 2018

Keywords:
Cervical spine morphology
Sensitivity analysis
Finite element analysis
Spine ligaments
Mesh morphing

ABSTRACT

Cervical spine finite element models reported in biomechanical literature usually represent a static morphology. Not considering morphology as a model parameter limits the predictive capabilities for applications in personalized medicine, a growing trend in modern clinical practice. The objective of the study was to investigate the influence of variations in spinal morphology on the flexion-extension responses, utilizing mesh-morphing-based parametrization and metamodel-based sensitivity analysis. A C5-C6 segment was used as the baseline model. Variations of intervertebral disc height, facet joint slope, facet joint articular processes height, vertebral body anterior-posterior depth, and segment size were parametrized. In addition, material property variations of ligaments were considered for sensitivity analysis. The influence of these variations on vertebral rotation and forces in the ligaments were analyzed. The disc height, segmental size, and body depth were found to be the most influential (in the cited order) morphology variations; while among the ligament material property variations, capsular ligament and ligamentum flavum influenced vertebral rotation the most. Changes in disc height influenced forces in the posterior ligaments, indicating that changes in the anterior load-bearing column of the spine could have consequences on the posterior column. A method to identify influential morphology variations is presented in this work, which will help automation efforts in modeling to focus on variations that matter. This study underscores the importance of incorporating influential morphology parameters, easily obtained through computed tomography/magnetic resonance images, to better predict subject-specific biomechanical responses for applications in personalized medicine.

1. Introduction

Although all the vertebrae in the human spinal column, apart from those in the caudal and cranial extremes, share a similar structure, each spinal region is distinct. The cervical spine segments differ from the thorax and lumbar segments with respect to their size and shape of vertebral components, particularly facet joints and transverse and posterior processes (Yoganandan et al., 2017). The morphology of the cervical vertebrae in itself, however, exhibits a range of variation with respect to age, stature, and sex (Klinich et al., 2004; Parenteau et al., 2014). Dissection and radiographic studies on the facet joints show variation in the articular surface slopes and articular process heights (Milne, 1991; Nowitzke et al., 1994; Panjabi et al., 1993; Penning, 1988; Putz, 1981). The intervertebral disc also exhibits considerable height variation (Gilad and Nissan, 1986). Even though male-to-female vertebral size variations can be expected due to differences in stature between the two groups, height-matched studies have shown significant ($p < 0.05$) differences, especially the anteroposterior vertebral depth of the cervical spine, which is lower in females than males (Stemper et al., 2008; Vasavada et al., 2008). A representative list of studies on the morphology variations in cervical spine components is given (Table 1).

Given the considerable variation in vertebral morphology, it is pertinent to consider morphology as input variables in finite element (FE) models, rather than as static input in the traditional and common spine FE modeling approach (Fagan et al., 2002; Kim et al., 2018; Suarez-Escobar and Rendon-Velez, 2017). Different approaches have been used to consider the influence of morphology. Earlier studies used models with simplified geometries to represent vertebral morphological variations (Maurel et al., 1997; Robin et al., 1994). Recent studies have focused on generating a population of models representing multiple individuals to capture inter-subject variabilities (Campbell et al., 2016; Laville

* Corresponding author at: Department of Engineering Design, Indian Institute of Technology Madras, Chennai 600 0036, India.
E-mail address: gsaravana@iitm.ac.in (G. Saravana Kumar).

https://doi.org/10.1016/j.jbiomech.2018.12.044
0021-9290/

Table 1
Morphological variations of major cervical spine components reported in literature.

Study (Sample size)	Study method		Morphology measurement	
Vertebral body depth (mm)				
Milne, 1991	Disarticulated Skeleton		Mean (SE)	
(N=61)			Male (n=40)	Female (n=21)
		C3	15.33 (0.23)	13.78 (0.16)
		C4	15.99 (0.29)	14.36 (0.30)
		C5	16.19 (0.29)	13.97 (0.19)
		C6	16.6 (0.27)	14.9 (0.53)
		C7	16.45 (0.25)	14.66 (0.27)
		T1	16.24 (0.24)	14.36 (0.31)
Vasavada et al., 2008	Lateral radiographs		Mean (SD)	
(N=14)	Height matched-pair volunteers		Male	Female
		C2	14.2 (1.0)	13.1 (1.0)
		C3	14.2 (1.6)	12.8 (0.8)
		C4	14.2 (1.2)	13.0 (1.0)
		C5	15.2 (1.1)	13.0 (0.9)
		C6	15.6 (1.0)	14.0 (1.0)
		C7	15.5 (1.3)	13.7 (1.2)
Facet Joint Height (mm)				
Putz, 1981	Disarticulated Vertebrae,		Mean (SD)	
(N=66)	Height with respect to endplates	C3	2.8 (2.3)	
		C4	5.4 (2.0)	
		C5	6.2 (2.0)	
		C6	7.0 (4.1)	
		C7	8.1 (2.4)	
		T1	7.0 (2.8)	
Penning, 1988	Lateral Radiograph,		Mean (Variation)	
(N=20)	measured from superior endplate	C3	4.9 (2–8)	
		C4	7.2 (4–10)	
		C5	9.3 (7–11)	
		C6	10.1 (8–13)	
		C7	11.6 (9–15)	
Panjabi et al., 1993	Disarticulated Vertebrae,		Mean (SE)	
(N=12)	Height with respect to superior endplates	C3	12.5 (1.1)	
		C4	12.3 (1.2)	
		C5	12.0 (1.1)	
		C6	11.2 (0.8)	
		C7	11.7 (0.6)	
		T1	12.6 (1.2)	
Nowitzke et al., 1994	Lateral Radiograph,		Mean (SD)	
(N=61)	measured from superior endplate	C3	6.2 (3.2)	
		C4	8.7 (2.6)	
		C5	10.2 (2.2)	
		C6	11.7 (3.0)	
		C7	13.6 (2.8)	
Facet Joint Slope (°)				
Penning, 1988	Lateral Radiograph	Slope	Mean (Variation)	
(N =20)	(with respect to posterior border of vertebral body)	C2-C3	45.2 (22–65)	
		C3-C4	48.6 (30–65)	
		C4-C5	48.7 (30–60)	
		C5-C6	46.3 (30–60)	
		C6-C7	38.1 (30–55)	
Milne, 1991	Disarticulated Skeleton		Mean (SE)	
(N= 61)	(with respect to superior endplate)	C2-C3	124.3 (0.89)	
		C3-C4	124.4 (0.65)	
		C4-C5	127.0 (0.70)	
		C5-C6	125.7 (0.72)	
		C6-C7	116.0 (0.69)	
		C7-T1	111.9 (0.75)	
Panjabi et al., 1993	Disarticulated Skeleton		Mean (SE)	
(N = 12)	(with respect vertebral transverse plane)	C2-C3	40.7 (4.7)	
		C3-C4	48.8 (3.1)	
		C4-C5	47.0 (4.6)	
		C5-C6	45.8 (2.9)	
		C6-C7	47.2 (2.8)	
		C7-T1	62.2 (2.6)	
Nowitzke et al., 1994	Lateral Radiographs		Mean (SD)	
(N = 44)	(with respect to local axis defined at posterior vertebral body edge)	C2-C3	36.4 (7.8)	
		C3-C4	40.3 (6.1)	
		C4-C5	41.7 (8.5)	
		C5-C6	39.7 (8.4)	
		C6-C7	31.4 (7.5)	

(*continued on next page*)

Table 1 (*continued*)

Study (Sample size)	Study method		Morphology measurement	
Disc Height (mm)				
Gilad and Nissan, 1986 (N=141)	Lateral radiographs		Anterior	Posterior
		C2-C3	4.8 ± 1.0	3.4 ± 1.0
		C3-C4	5.3 ± 0.9	3.3 ± 0.9
		C4-C5	5.5 ± 1.0	3.0 ± 1.0
		C5-C6	5.4 ± 1.0	3.0 ± 0.9
		C6-C7	5.2 ± 1.0	3.0 ± 1.0

et al., 2009; Xu et al., 2017). Sensitivity studies on lumbar motion segments evaluated the influence of spinal variations (Meijer et al., 2011; Niemeyer et al., 2012). The methods used for the above-mentioned studies varied from parametric models using simplified geometry (Niemeyer et al., 2012) to statistical shape models using automated morphing techniques (Alvarez and Kleiven, 2018; Campbell and Petrella, 2016). Morphology and material property were considered together for sensitivity analysis in a recent study (Zander et al., 2017), and spinal curvature and facet joint gap were considered as morphological parameters in the cited study.

It is important to identify the influential morphological variations to better predict responses of the spine, especially in patient/subject-specific models. The objective of the present study is, therefore, to determine the contributions of cervical spine morphology variations, along with spinal ligament material property variations, to intervertebral rotational responses and ligament forces, using a single-motion segment FE model of the lower cervical spine.

2. Methods

This study involved three steps: development of the baseline FE model of the cervical spine segment, implementation of mesh morphing to parametrize the spine morphology, and sensitivity analysis using metamodeling to evaluate the contribution of the morphological variations.

2.1. Finite element model of cervical spine segment

An FE model of a male C5-C6 spine segment was developed to be used as the baseline model. The spinal components were meshed using hexahedral/quadrilateral elements (Fig. 1). Element quality thresholds used in this study were aspect ratio < 5 and Jacobian > 0.5 for hexahedral elements and aspect ratio < 5 and Jacobian > 0.7 for quadrilateral elements. The cancellous bone of the vertebral structures was modeled using hexahedral elements, while the cortical structure was modeled using shell elements (Panjabi et al., 2001a, 2001b). The facet joint definitions included the articular cartilage and capsular ligaments between the bilateral articular processes. The extent of the facet cartilage on the articular surfaces were defined from facet morphology study based on cryomicrotome images (Yoganandan et al., 2003). Penalty-based frictionless contact was defined for the vertebrae and articular surfaces. The material parameter definitions are given in Table 2.

The intervertebral disc was modeled as two distinct regions: annulus and nucleus. The annulus consisted of the ground substance and fiber definitions. The ground substance was a hyperelastic foam defined using Hill strain energy function (Panzer and Cronin, 2009). The fibers were defined using membrane elements with tension-only directional fibers embedded in the ground substance (Östh et al., 2016). The fibers in the anterior annulus region were defined in a crisscross manner, while fibers in the posterior region were defined in the vertical direction. The anterior annulus fibers did not form a continuous ring with the posterior annulus fibers, forming a gap bilaterally at the uncovertebral clefts. The uncovertebral clefts, unique to cervical spine segments, are devoid of fibers (Appendix A1) (Mercer and Bogduk, 1999). The nucleus was meshed with a posteriorly displaced position (Fig. 1) to account for the anteroposterior asymmetry of the annulus in the human cervical spine (Mercer and Bogduk, 1999; Tonetti et al., 2005). The nucleus material was defined as an incompressible fluid with a bulk modulus of 1720 MPa (Iatridis et al., 1996; Skrzypiec et al., 2007).

The anterior longitudinal ligament (ALL), posterior longitudinal ligament (PLL), capsular ligament (CL), ligamentum flavum (LF),

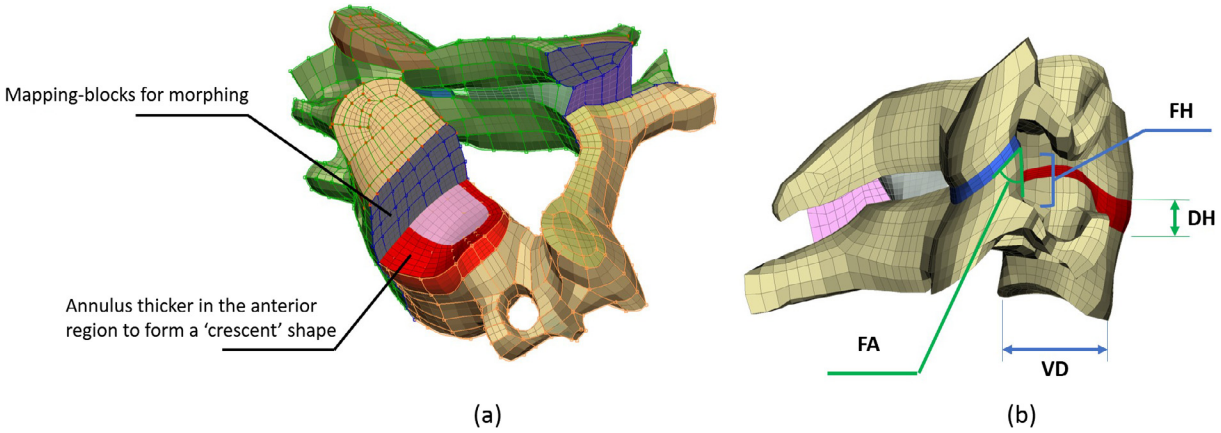

Fig. 1. (a) Cut-cross section of C5-C6 segment FE model showing the asymmetric structure of cervical annulus, mapping blocks used for mesh morphing and ligaments represented as membrane elements. (b) The vertebral morphological variations parametrized in this study. FA: Facet Angle, VD: Vertebral Body Depth, DH: Disc height, FH: Facet articular processes height.

Table 2
Material parameters of spinal components.

Component	Element type	Constitutive model	Parameters	Reference
Cortical bone	Quadrilateral shell	Linear elastic	E = 16.8 GPa, ν = 0.3	Reilly and Burstein (1975)
Trabecular bone	Hexahedral solid	Linear elastic	E = 400 MPa ν = 0.3	Kopperdahl and Keaveny (1998), Yoganandan et al. (2006)
Annulus ground substance	Hexahedral solid	Hill Foam	n = 2, C_1 = 0.115 MPa C_2 = 2.101 MPa C_3 = −0.893 MPa b_1 = 4, b_2 = −1, b_1 = -2	Iatridis et al. (1998), Panzer and Cronin (2009)
Annulus fibrosus	Quadrilateral membrane	Orthotropic nonlinear elastic	Fiber angle (45–60°)	Cassidy et al. (1989), Holzapfel et al. (2005)
Nucleus pulposus	Hexahedral solid	Fluid	K = 1720 MPa	Skrzypiec et al. (2007), Yang and Kish (1988)
Endplate	Quadrilateral shell	Linear elastic	E = 5.6 GPa, ν = 0.3	Panzer and Cronin (2009)
Facet cartilage	Quadrilateral shell	Linear elastic	E = 10 MPa, ν = 0.3	Yamada (1970)
Ligaments	Quadrilateral membrane	Non-linear stress-strain curves		Mattucci et al. (2012), Yoganandan et al. (2000)

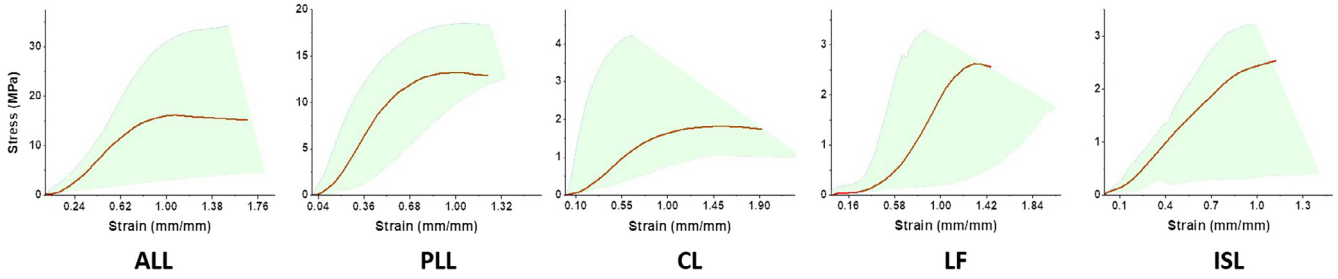

Fig. 2. Shaded region shows the range of stress-strain variations in cervical spine ligaments, calculated from load-displacement curves reported in Mattucci et al. (2012). The red line shows the average response as given in Mattucci et al. 2015, which was used to define ligament properties in the baseline model of the present study. (For interpretation of the references to color in this figure legend, the reader is referred to the web version of this article.)

and interspinous ligament (ISL) were defined as quadrilateral non-linear orthotropic membrane elements, with no resistance in compression. The ligaments' points of attachment were modeled based on anatomical studies (Mercer and Bogduk, 1999; Yoganandan et al., 2000). The points of attachment of the anterior and posterior longitudinal ligaments were along the anterior and posterior surfaces of the vertebral bodies. The capsular ligaments were attached between the articular processes, ligamentum flavum between the laminae, and interspinous ligament between the spinous processes. The second Piola-Kirchoff stress-Green strain definition describing the ligaments (Fig. 2) was derived from quasi-static experimental force-displacement responses (Mattucci and Cronin, 2015). Transverse in-plane property of the ligament membranes were defined by scaling the stress by a factor of 0.1 (Östh et al., 2016). Sagittal quasi-static moment loads of up to 3 Nm in flexion and extension were applied on the nodes on the superior surface of the C5 vertebra. The inferior nodes of C6 vertebra were constrained in all degrees of freedom. The models were simulated on LS DYNA R8.1.0 (LSTC).

2.2. Morphology and ligament property parametrization

Disc height, facet joint slope, facet joint articular processes height, anteroposterior vertebral depth, and segment size variations were parametrized on the baseline model (Table 3). The disc height was varied by 1.4 mm (Gilad and Nissan, 1986). The facet angle was varied by 6°, and facet articular process height was varied by 2 mm (Milne, 1991; Nowitzke et al., 1994; Panjabi et al., 1993; Penning, 1988; Putz, 1981). A 10% variation in the vertebral depth was considered, and it was based on the male-female differences reported in a height-matched study (Vasavada et al., 2008). In addition to these local/non-uniform variations, the overall size of the segment was varied by ±5% to account for the vertebral variations reported in a published head-circumference-matched study (Stemper et al., 2008).

For the parametrization of the above morphological variations on the baseline model, the vertebral shape was discretized with interconnected blocks of simpler shape acting as mapping-blocks (Fig. 1). The vertices of each block acted as the control points for

Table 3
Morphology and ligament property variations considered as parameters in this study.

Morphology			Ligament				
Parameter	Mean	Variation	Ligament	Stress scale		Strain scale	
				Max	Min	Max	Min
Disc height	4.8 mm	±0.7 mm	Anterior Longitudinal	+40%	−50%	+50%	−20%
Facet angle	36.6°	±3°	Posterior Longitudinal	+60%	−40%	+40%	−50%
Facet height	9.6 mm	±1 mm	Capsular	+100%	−50%	+50%	−50%
Vertebral body depth	15.8 mm	±0.75 mm	Ligamentum Flavum	+50%	−50%	+50%	−25%
Segment size		±5%	Interspinous	+25%	−25%	+50%	−25%

the FE nodes encompassed within. The new positions of FE nodes for modified morphology were obtained using linear interpolation based on the coordinates of control points. The parameters of morphology variation given in Table 3 were implemented by defining affine transformations of control points corresponding to respective spinal components. The accuracy of mesh morphing depends on the number and spacing of the control points in the three-dimensional space of the FE model (Jolivet et al., 2015; Zhang et al., 2017). Using mapping-blocks aided in the distribution of control points uniformly throughout the irregular shape of the vertebra and ensured good quality mesh after morphing. Mesh morphing routines in FE preprocessor ANSA 17.1.0 (BETA CAE Systems) were used to implement the morphological variations.

For the ligament properties, the baseline model definitions were based on the mean curve from quasi-static testing of cervical spine ligaments (Mattucci and Cronin, 2015). The ligaments' stress-strain properties were scaled (Table 3) and constrained within the maximum and minimum ligament responses as shown in Fig. 2.

2.3. Sensitivity analysis

The sensitivity analysis was performed in two steps. In the first step, the morphological and ligament parameters were considered separately for screening using regression-based ANOVA on the normalized parameter space. Three-level D-Optimal method was used for the point selection in this step. Parameters with more than 10% influence on vertebral rotation were considered for the next step. In the second step, the morphological and ligament parameters identified from the initial screening were considered for a metamodel-based global sensitivity analysis. A randomized experimental design using maximin Latin-Hypercube sampling (LHS) was used for design point selection, and a radial-basis function network with multi-quadric functions was used to generate metamodels for flexion and extension simulation responses (Park and Sandberg, 1991). Sobol's global sensitivity indices for parameters were evaluated on the metamodels (Sobol and Kucherenko, 2005). Along with the Sobol's indices, correlation analysis was used to determine if they were positively or negatively correlated with the outputs and to determine any dependency on the magnitude of applied moments. The influence of the parameters on ligament forces was investigated using correlation analysis. The details of sensitivity analysis—including the experimental design and metamodeling—are given in Appendix A2.

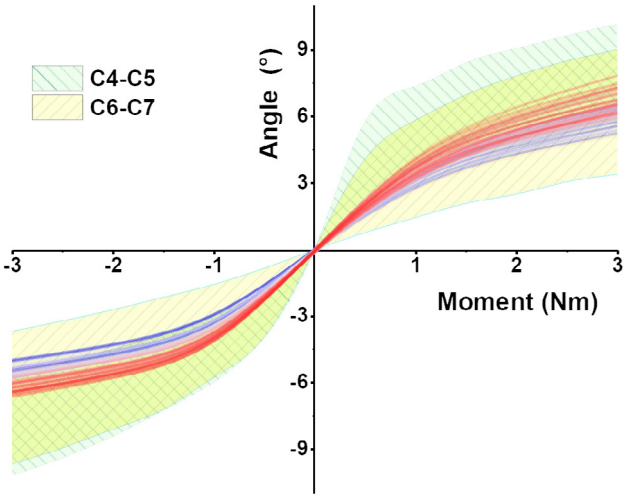

Fig. 3. Flexion-extension response of the models with the morphological and ligament property variations (where positive moment and vertebral rotation indicate flexion). The shaded region shows experimental corridors from male cervical spine segments (Nightingale et al., 2007). Response variation is shown in terms of the most influential morphology parameter, disc height. Red line indicates maximum disc height, and blue line indicates minimum disc height, with transition showing intermediate disc height values based on the Latin-hypercube sampling. (For interpretation of the references to color in this figure legend, the reader is referred to the web version of this article.)

3. Results

In the first step of sensitivity analysis, 10 models were generated for variations in morphological parameters, and 20 models were generated for variations in ligament property parameters. Considering flexion and extension, disc height, segment size, and vertebral depth, and ligament parameters of ALL stress scale factor, CL stress and strain scale factors, and LF stress and strain scale factors were identified for the second step of the analysis. The regression coefficients of the parameters in the first level screening are given in the Appendix (Figs. A1 and A2). These parameters were used to generate 70 models in the second step of combined morphology-ligament variations using the LHS. The vertebral rotation responses of these models with morphological and ligament material property variations are shown in Fig. 3. The changes in vertebral rotation due to these variations was 2.7° in flexion and 1.7° in extension.

Metamodels were constructed from the flexion and extension responses of the 70 models. The contribution of the parameters to vertebral rotation, in terms of Sobol's sensitivity indices and correlation coefficients, is shown in Fig. 4. The Sobol's sensitivity indices, expressed as percentage of total variation, were evaluated on the metamodels for vertebral rotation at 3 Nm loading. The correlation coefficients were evaluated for vertebral rotations at 1 Nm, 2 Nm, and 3 Nm. In flexion, the disc height was the most influential parameter, followed by the scale factors of LF and CL strain (Fig. 4 (a)). This was closely followed by the segment size and vertebral depth. While the influence of most parameters was independent of the moment magnitude, the influence of LF strain scale factor increased with an increase in moment, while the influence of segment size reduced with increase in size. In extension, the disc height variations were the most influential, followed by smaller contributions from the vertebral depth and segment size (Fig. 4 (b)).

The influence of the variations on forces resisted by posterior ligaments in flexion and ALL in extension at 3 Nm is shown in Fig. 5. An increase in the ligament stress scale factors tended to increase the forces resisted by the ligaments, while the increase in the strain scale factors tended to reduce the forces resisted in the ligaments. These changes influenced not only the respective ligaments but inversely affected the forces resisted by the other ligaments. The morphological variations also influenced the forces resisted by ligaments: variations in the disc height influenced forces in the longitudinal ligaments and ISL, while variations in the segment size and vertebral depth slightly influenced the forces in LF. The following were the range of variations in the forces: ALL 16.8 N to 5.12 N, PLL 56 N to 7.9 N, CL 105.6N to 13.9 N, LF 61.3 N to 7.1 N, and ISL 27.8 N to 12.3 N.

4. Discussion

The aim of this study was to determine the influence of morphological and ligament property variations on cervical spine sagittal bending responses using a FE analysis. As the FE model in this study represented a male cervical spine segment, the simulation responses were compared and validated with the experimental responses of male segments (Nightingale et al., 2007). The C5-C6 responses in the current study were compared with C4-C5 and C6-C7 responses, because the cited study did not con-

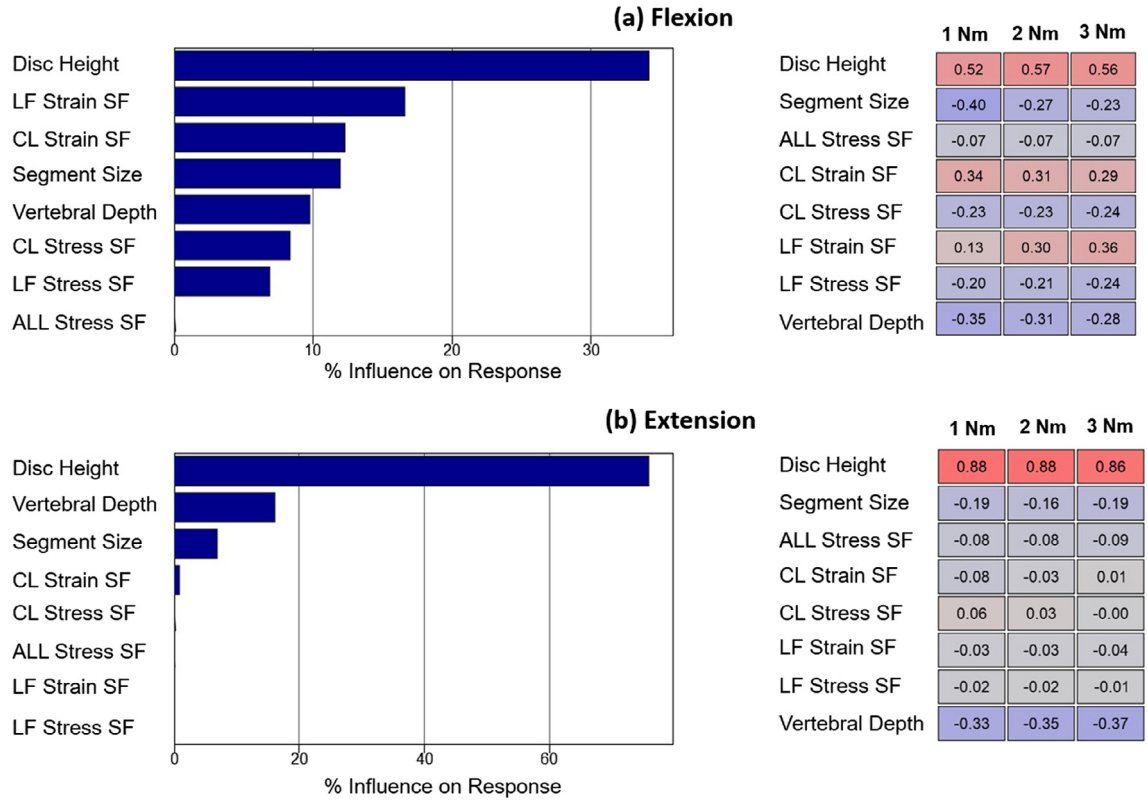

Fig. 4. Contributions of morphology and ligament property parameters to variations in vertebral rotational responses in flexion and extension. (Left) Sensitivity of parameters at 3 N m moment load, in terms of Sobol's Global Sensitivity Indices (Right) Correlation coefficients of parameters at 1 N m, 2 N m, 3 N m moment loads.

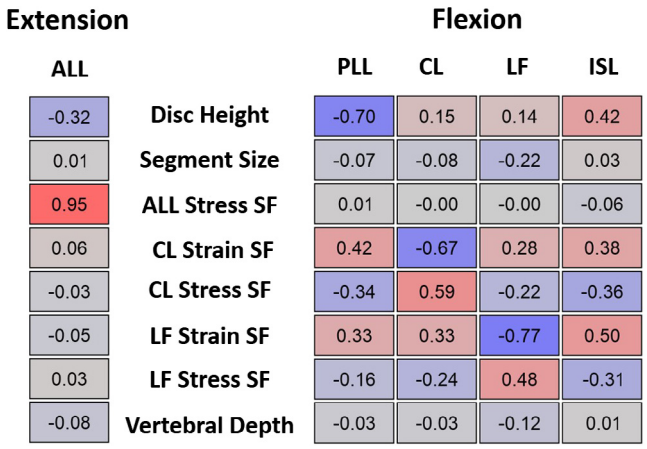

Fig. 5. Correlation coefficients, showing influence of parameters on ligament forces. Forces in the posterior ligaments in flexion and anterior ligament in extension are given.

duct experiments using the C5-C6 segment. The lower cervical spine segments have overlapping response corridors as they share a similar morphology (Fig. 3). Cervical intervertebral discs do not form annulus concentric lamellae as in the lumbar region (Mercer and Bogduk, 1999) and this is the first cervical spine FE model, to the authors' knowledge, that has captured this distinctiveness. The dissimilarity of structure between the anterior and posterior regions can have implications on the endplate stress distributions, non-symmetric flexion-extension behavior of the cervical spine segments, and responses of the degenerative spine (John et al., 2017; Tonetti et al., 2005).

Mesh-morphing techniques have been instrumental in expedited development of subject-specific spine models from validated baseline models with age and gender variations, as well as various degenerative conditions (Alvarez and Kleiven, 2018; Campbell et al., 2016; Hadagali et al., 2018). The present study used a mapping-block-based morphing to parametrize morphology. This method was previously shown to result in negligible morphing-related mesh quality deterioration (John et al., 2018). For the ligament properties, stresses and strains were scaled in the same manner as soft tissue parameters in previous studies (Zander et al., 2017). A two-step sensitivity analysis was used to reduce the parameter space dimension and, hence, reduce the number of simulations required for the global sensitivity analysis. When compared with the C4-C5 experimental responses, the total variation in model response was 73% and 48% of the flexion and extension experimental corridors, respectively. The remainder of response variations in the experimental corridors could be attributed to other anatomical parameters, including the intervertebral disc material property, which were not considered in this study.

4.1. Influence on vertebral rotation

The vertebral rotation for a given moment indicates the stiffness of the spinal motion segment, the variation of which was evaluated in terms of morphological and material changes in the intervertebral region. Disc height was found to be the morphology with the greatest contribution to variations in vertebral rotation: 34% in flexion and 76% in extension. A reduction in the disc height resulted in the stiffening of the motion segment. As loss of disc height is part of the natural disc degeneration process, this reduction may explain the stiffening of cervical spine segments with aging (Pan et al., 2018). The vertebral body depth, which is reported to be gender-dependent by some studies (Stemper et al., 2008; Vasavada et al., 2008), was found to have smaller contributions of 10% and 16% in flexion and extension, respectively. An

increase in these parameters resulted in the decrease of vertebral rotation (Fig. 4).

The flexion vertebral rotation was influenced by strain scaling in the capsular ligament and ligamentum flavum (17% and 12%, respectively). An increase in the strain scaling resulted in an increase in vertebral rotation. This can be attributed to an increase in the toe region when the strain axis is scaled positively, resulting in reduced resistance to flexion by these posterior ligaments. The influence of capsular ligaments strain scaling remained constant, while that of the ligamentum flavum increased with flexion magnitudes. This can be attributed to the ligament response shifting to the stiffer, linear portion ligament force-displacement curve and the greater moment arm of ligamentum flavum compared to the capsular ligaments. Although the facet angle and facet joint height ranges did not have considerable influence on the vertebral rotation for magnitudes of moments considered in this study (Fig. A1), this may not be the case at higher load levels, when the opposing articular surfaces may make contact in extension. At the present moment levels, the material property variations in the facet capsular ligament variations were more influential than the facet morphology variations.

4.2. Influence on ligament forces

The forces resisted by the ligaments were influenced by both the morphological and ligament material parameters. Among the morphological variations, disc height contributed the most to variations in forces resisted by the ligaments. This influence was different for the longitudinal ligaments (ligaments attached to the vertebral body) and the posterior ligaments (Fig. 5). An increase in the disc height resulted in the longitudinal ligaments resisting less loads, while an increase in disc height increased the forces resisted by the posterior ligaments, especially the interspinous ligament. This shows that changes in the anterior load-bearing column of the spine, of which disc is the major component, can have implications on the structural responses of the posterior load-bearing column. For example, disc degenerative changes can be expected to change the load paths in the posterior and articular processes.

The forces resisted by a ligament was influenced by both the stress and strain scale factors. An increase in strain scale factor resulted in a decrease in force resisted by the ligament, which can be explained by the lengthening of the ligament toe region due to strain scaling. On the other hand, the forces resisted by the ligaments were positively correlated with the stress scale factor, which can be explained by the increase in ligament stiffness due to stress scaling. The force resisted in the ligaments other than the one under consideration exhibited an opposite trend. This can be attributed to compensation reaction in these ligaments. For example, an increase in the strain scale factor in the LF resulted in a lower force being resisted by this ligament, while it resulted in the other ligaments resisting more force to compensate for the loss of stiffness. This pattern of response shows how degenerative changes or injurious changes in one ligament can influence the responses in other spinal ligaments also.

Since geometric and material nonlinearities vary with the magnitude of loading, the contributions of these biological variations also vary with the magnitude (Fig. 4). Therefore, it is important to evaluate the contribution of variations at different loads as done in this study. In the present investigation, the posterior ligaments influenced the flexion response more at higher moments, while the influence of size variations was greater at lower-level moments. In addition to the mode of loading (flexion or extension), the influence of variations being a function of the magnitude of loads, extrapolating FE model sensitivities to load levels other than the ones studied should be done with caution. The present study simulated loads up to 3 N m moment as performed by the experiments of Nightingale et al. (2007). It should be noted that physiological loading tests by many researchers have used a lower level, up to 2 N m (Kallemeyn et al., 2010; Panjabi et al., 2001b; Wheeldon et al., 2006). This study was limited to flexion and extension loading modes. The contribution of the facet joint variations was negligible in the flexion and extension loading modes for the magnitudes of load levels considered in this study. The role of the facet joint variations, however, may be more in lateral bending and axial rotation because of their expected additional engagement in these loading modes.

Many studies are focused on lumbar spine (Niemeyer et al., 2012). Although cervical and lumbar spine are similar, cervical spine segments have a unique morphology especially in the facet joints, and posterior and transverse process. In addition, their loading conditions are unique, for example, suboccipital headaches and neck and shoulder pain from whiplash loading. The development of parametrized cervical spine FE model was motivated by these reasons. To the authors' best knowledge, this is the first detailed cervical spine with parametrized morphology for sensitivity analysis.

In summary, using a parametrized finite element model of a lower cervical spine segment, this study investigated the role of morphology and ligament property variations on the vertebral rotation and ligament forces in sagittal bending. The disc height was the most influential morphological variation, followed by the segment size and vertebral depth. This finding correlates with previous studies on the lumbar spine morphological variations (Meijer et al., 2011; Niemeyer et al., 2012). Among the ligament variations, the capsular ligament and ligamentum flavum properties had the most influence on vertebral rotation. This paper presented a methodology to identify influential morphological variations, making it possible for model automation efforts to focus only on the variations that influence model outputs. As patient-specific morphological properties can be easily obtained through computed tomography/magnetic resonance images, the present study underscores the importance of incorporating influential morphology variations to better predict subject-specific biomechanical responses for applications in personalized medicine.

Conflict of interest

None of the authors have any disclosures.

Acknowledgement

This work was undertaken as part of research funded by Office of the Assistant Secretary of Defence for Health Affairs, USA (Award No. W81XWH-16-01-0010), and the use of the facilities at the Zablocki VA Medical Center, Milwaukee, Wisconsin, USA. The authors would like to thank Drs. Mike Arun and Jamie Baisden for their assistance. The third author, Narayan Yoganandan, is an employee of the Medical Centre. Any views expressed herein are those of the authors and not necessarily representative of the funding organizations.

Appendix A. Supplementary material

Supplementary data to this article can be found online at https://doi.org/10.1016/j.jbiomech.2018.12.044.

References

Alvarez, V.S., Kleiven, S., 2018. Effect of pediatric growth on cervical spine kinematics and deformations in automotive crashes. J. Biomech. 71, 76–83. https://doi.org/10.1016/j.jbiomech.2018.01.038.

Campbell, J.Q., Coombs, D.J., Rao, M., Rullkoetter, P.J., Petrella, A.J., 2016. Automated finite element meshing of the lumbar spine: verification and validation with 18 specimen-specific models. J. Biomech. 49, 2669–2676. https://doi.org/10.1016/j.jbiomech.2016.05.025.

Campbell, J.Q., Petrella, A.J., 2016. Automated finite element modeling of the lumbar spine: using a statistical shape model to generate a virtual population of models. J. Biomech. 49, 2593–2599. https://doi.org/10.1016/j.jbiomech.2016.05.013.

Cassidy, J.J., Hiltner, A., Baer, E., 1989. Hierarchical Structure of the Intervertebral Disc. Connect. Tissue Res. 23, 75–88. https://doi.org/10.3109/03008208909103905.

Fagan, M.J., Julian, S., Mohsen, A.M., 2002. Finite element analysis in spine research. Proc. Inst. Mech. Eng. Part H J. Eng. Med. 216, 281–298. https://doi.org/10.1243/09544110260216568.

Gilad, I., Nissan, M., 1986. A study of vertebra and disc geometric relations of the human cervical and lumbar spine. Spine (Phila. Pa. 1976). 11, 154–157. https://doi.org/10.1097/00007632-198603000-00010.

Hadagali, P., Peters, J.R., Balasubramanian, S., 2018. Morphing the feature-based multi-blocks of normative/healthy vertebral geometries to scoliosis vertebral geometries: development of personalized finite element models. Comput. Methods Biomech. Biomed. Eng. 21, 297–324. https://doi.org/10.1080/10255842.2018.1448391.

Holzapfel, G.A., Schulze-Bauer, C.A.J.J., Feigl, G., Regitnig, P., 2005. Single lamellar mechanics of the human lumbar anulus fibrosus. Biomech. Model. Mechanobiol. 3, 125–140. https://doi.org/10.1007/s10237-004-0053-8.

Iatridis, J.C., Setton, L.a., Foster, R.J., Rawlins, B.A., Weidenbaum, M., Mow, V.C., 1998. Degeneration affects the anisotropic and nonlinear behaviors of human anulus fibrosus in compression. J. Biomech. 31, 535–544.

Iatridis, J.C., Weidenbaum, M., Setton, L.A., Mow, V.C., 1996. Is the nucleus pulposus a solid or a fluid? Mechanical behaviors of the nucleus pulposus of the human intervertebral disc. Spine (Phila. Pa. 1976). 21, 1174–1184.

John, J.D., Arun, M.W.J., Saravanakumar, G., Yoganandan, N., 2017. Cervical spine finite element model with anatomically accurate asymmetric intervertebral discs. Summer Biomechanics, Bioengineering, and Biotransport Conference.

John, J.D., Yoganandan, N., Arun, M.W.J., Saravana Kumar, G., 2018. Influence of morphological variations on cervical spine segmental responses from inertial loading. Traffic Inj. Prev. 19, S29–S36. https://doi.org/10.1080/15389588.2017.1403017.

Jolivet, E., Lafon, Y., Petit, P., Beillas, P., 2015. Comparison of Kriging and moving least square methods to change the geometry of human body models. Stapp Car Crash J. 59, 337–357.

Kallemeyn, N., Gandhi, A., Kode, S., Shivanna, K., Smucker, J., Grosland, N., 2010. Validation of a C2–C7 cervical spine finite element model using specimen-specific flexibility data. Med. Eng. Phys. 32, 482–489. https://doi.org/10.1016/j.medengphy.2010.03.001.

Kim, Y.H., Khuyagbaatar, B., Kim, K., 2018. Recent advances in finite element modeling of the human cervical spine. J. Mech. Sci. Technol. 32, 1–10. https://doi.org/10.1007/s12206-017-1201-2.

Klinich, K.D., Ebert, S.M., Van Ee, C.A., Flannagan, C.A.C., Prasad, M., Reed, M.P., Schneider, L.W., 2004. Cervical spine geometry in the automotive seated posture: variations with age, stature, and gender. Proc. 48th Stapp Car Crash Conf. Nashv. Tennessee 48, 301–330 [pii].

Kopperdahl, D.L., Keaveny, T.M., 1998. Yield strain behavior of trabecular bone. J. Biomech. 31, 601–608. https://doi.org/10.1016/S0021-9290(98)00057-8.

Laville, A., Laporte, S., Skalli, W., 2009. Parametric and subject-specific finite element modelling of the lower cervical spine. Influence of geometrical parameters on the motion patterns. J. Biomech. 42, 1409–1415. https://doi.org/10.1016/j.jbiomech.2009.04.007.

Mattucci, S.F.E., Cronin, D.S., 2015. A method to characterize average cervical spine ligament response based on raw data sets for implementation into injury biomechanics models. J. Mech. Behav. Biomed. Mater. 41, 251–260. https://doi.org/10.1016/j.jmbbm.2014.09.023.

Mattucci, S.F.E., Moulton, J.A., Chandrashekar, N., Cronin, D.S., 2012. Strain rate dependent properties of younger human cervical spine ligaments. J. Mech. Behav. Biomed. Mater. 10, 216–226. https://doi.org/10.1016/j.jmbbm.2012.02.004.

Maurel, N., Lavaste, F., Skalli, W., 1997. A three-dimensional parameterized finite element model of the lower cervical spine, study of the influence of the posterior articular facets. J. Biomech. 30, 921–931. https://doi.org/10.1016/S0021-9290(97)00056-0.

Meijer, G.J.M.M., Homminga, J., Veldhuizen, A.G., Verkerke, G.J., 2011. Influence of interpersonal geometrical variation on spinal motion segment stiffness. Spine (Phila. Pa. 1976). 36, E929–E935. https://doi.org/10.1097/BRS.0b013e3181fd7f7f.

Mercer, S., Bogduk, N., 1999. The ligaments and annulus fibrosus of human adult cervical intervertebral discs. Spine (Phila. Pa. 1976).

Milne, N., 1991. The role of zygapophysial joint orientation and uncinate processes in controlling motion in the cervical spine. J. Anat. 178, 189–201.

Niemeyer, F., Wilke, H.-J., Schmidt, H., 2012. Geometry strongly influences the response of numerical models of the lumbar spine—a probabilistic finite element analysis. J. Biomech. 45, 1414–1423. https://doi.org/10.1016/j.jbiomech.2012.02.021.

Nightingale, R.W., Carol Chancey, V., Ottaviano, D., Luck, J.F., Tran, L., Prange, M., Myers, B.S., 2007. Flexion and extension structural properties and strengths for male cervical spine segments. J. Biomech. 40, 535–542. https://doi.org/10.1016/j.jbiomech.2006.02.015.

Nowitzke, A., Westaway, M., Bogduk, N., 1994. Cervical zygapophyseal joints: geometrical parameters and relationship to cervical kinematics. Clin. Biomech. 9, 342–348. https://doi.org/10.1016/0268-0033(94)90063-9.

Östh, J., Brolin, K., Svensson, M.Y., Linder, A., 2016. A female ligamentous cervical spine finite element model validated for physiological loads. J. Biomech. Eng. 138, 061005. https://doi.org/10.1115/1.4032966.

Pan, F., Arshad, R., Zander, T., Reitmaier, S., Schroll, A., Schmidt, H., 2018. The effect of age and sex on the cervical range of motion – a systematic review and meta-analysis. J. Biomech. 75, 13–27. https://doi.org/10.1016/j.jbiomech.2018.04.047.

Panjabi, M.M., Chen, N.C., Shin, E.K., Wang, J.L., 2001a. The cortical shell architecture of human cervical vertebral bodies. Spine (Phila Pa 1976) 26, 2478–2484. https://doi.org/10.1097/00007632-200111150-00016.

Panjabi, M.M., Crisco, J.J., Vasavada, A., Oda, T., Cholewicki, J., Nibu, K., Shin, E., 2001b. Mechanical properties of the human cervical spine as shown by three-dimensional load-displacement curves. Spine (Phila. Pa. 1976). 26, 2692–2700. https://doi.org/10.1097/00007632-200112150-00012.

Panjabi, M.M., Oxland, T., Takata, K., Goel, V., Duranceau, J., Krag, M., 1993. Articular facets of the human spine. Quantitative three-dimensional anatomy. Spine (Phila. Pa. 1976). 18, 1298–1310. https://doi.org/10.1097/00007632-199308000-00009.

Panzer, M.B., Cronin, D.S., 2009. C4–C5 segment finite element model development, validation, and load-sharing investigation. J. Biomech. 42, 480–490. https://doi.org/10.1016/j.jbiomech.2008.11.036.

Parenteau, C.S., Wang, N.C., Zhang, P., Caird, M.S., Wang, S.C., 2014. Quantification of pediatric and adult cervical vertebra-anatomical characteristics by age and gender for automotive application. Traffic Inj. Prev. 15, 572–582. https://doi.org/10.1080/15389588.2013.843774.

Park, J., Sandberg, I.W., 1991. Universal approximation using radial-basis-function networks. Neural Comput. 3, 246–257. https://doi.org/10.1162/neco.1991.3.2.246.

Penning, L., 1988. Differences in anatomy, motion, development and aging of the upper and lower cervical disk segments. Clin. Biomech. 3, 37–47. https://doi.org/10.1016/0268-0033(88)90124-6.

Putz, R., 1981. Funktionelle Anatomie der Wirbelgelenke, Normale und pathologische Anatomie. Georg Thiem Verlag, Stuttgart.

Reilly, D.T., Burstein, A.H., 1975. The elastic and ultimate properties of compact bone tissue. J. Biomech. 8 (6), 397–405. https://doi.org/10.1016/0021-9290(75)90075-5.

Robin, S., Skalli, W., Lavaste, F., 1994. Influence of geometrical factors on the behavior of lumbar spine segments: a finite element analysis. Eur. Spine J. 3, 84–90. https://doi.org/10.1007/BF02221445.

Skrzypiec, D.M., Pollintine, P., Przybyla, A., Dolan, P., Adams, M.A., 2007. The internal mechanical properties of cervical intervertebral discs as revealed by stress profilometry. Eur. Spine J. 16, 1701–1709. https://doi.org/10.1007/s00586-007-0458-z.

Sobol, I.M., Kucherenko, S.S., 2005. Global sensitivity indices for nonlinear mathematical models. Review. Wilmott 2005, 56–61. https://doi.org/10.1002/wilm.42820050114.

Stemper, B.D., Yoganandan, N., Pintar, F.A., Maiman, D.J., Meyer, M.A., DeRosia, J., Shender, B.S., Paskoff, G., 2008. Anatomical gender differences in cervical vertebrae of size-matched volunteers. Spine (Phila. Pa. 1976). 33, 44–49. https://doi.org/10.1097/BRS.0b013e318160462a.

Suarez-Escobar, M., Rendon-Velez, E., 2017. A survey on static and quasi-static finite element models of the human cervical spine. Int. J. Interact. Des. Manuf. 12, 741–765. https://doi.org/10.1007/s12008-017-0431-y.

Tonetti, J., Potton, L., Riboud, R., Peoc'h, M., Passagia, J.G., Chirossel, J.P., 2005. Morphological cervical disc analysis applied to traumatic and degenerative lesions. Surg. Radiol. Anat. 27, 192–200. https://doi.org/10.1007/s00276-004-0309-0.

Vasavada, A.N., Danaraj, J., Siegmund, G.P., 2008. Head and neck anthropometry, vertebral geometry and neck strength in height-matched men and women. J. Biomech. 41, 114–121. https://doi.org/10.1016/j.jbiomech.2007.07.007.

Wheeldon, J.A., Pintar, F.A., Knowles, S., Yoganandan, N., 2006. Experimental flexion/extension data corridors for validation of finite element models of the young, normal cervical spine. J. Biomech. 39, 375–380. https://doi.org/10.1016/j.jbiomech.2004.11.014.

Xu, M., Yang, J., Lieberman, I.H., Haddas, R., 2017. Lumbar spine finite element model for healthy subjects: development and validation. Comput. Methods Biomech. Biomed. Eng. 20, 1–15. https://doi.org/10.1080/10255842.2016.1193596.

Yamada, H., 1970. Strength of Biological Materials. Williams & Wilkins.

Yang, K.H., Kish, V.L., 1988. Compressibility measurement of human intervertebral nucleus pulposus. J. Biomech. 21, 865. https://doi.org/10.1016/0021-9290(88)90059-0.

Yoganandan, N., Arun, M.W.J., Dickman, C.A., Benzel, E.C., 2017. Practical anatomy and fundamental biomechanics. In: Steinmetz, M.P., Benzel, E.C. (Eds.), Benzel's Spine Surgery: Techniques, Complication Avoidance, and Management. Elsevier Inc.

Yoganandan, N., Knowles, S.A., Maiman, D.J., Pintar, F.a., 2003. Anatomic study of the morphology of human cervical facet joint. Spine (Phila. Pa. 1976). 28, 2317–2323. https://doi.org/10.1097/01.BRS.0000085356.89103.A5.

Yoganandan, N., Kumaresan, S., Pintar, F.A., 2000. Geometric and mechanical properties of human cervical spine ligaments. J. Biomech. Eng. 122, 623. https://doi.org/10.1115/1.1322034.

Yoganandan, N., Pintar, F.A., Stemper, B.D., Baisden, J.L., Aktay, R., Shender, B.S., Paskoff, G., Laud, P., 2006. Trabecular bone density of male human cervical and

lumbar vertebrae. Bone 39, 336–344. https://doi.org/10.1016/j.bone.2006.01.160.

Zander, T., Dreischarf, M., Timm, A.-K., Baumann, W.W., Schmidt, H., 2017. Impact of material and morphological parameters on the mechanical response of the lumbar spine – a finite element sensitivity study. J. Biomech. 53, 185–190. https://doi.org/10.1016/j.jbiomech.2016.12.014.

Zhang, K., Cao, L., Fanta, A., Reed, M.P., Neal, M., Wang, J.T., Lin, C.H., Hu, J., 2017. An automated method to morph finite element whole-body human models with a wide range of stature and body shape for both men and women. J. Biomech. 60, 253–260. https://doi.org/10.1016/j.jbiomech.2017.06.015.